View Article Online
DOI: 10.1039/C8DT04639E

Dalton Transaction

FRONTIER

Copper hydride clusters in energy storage and conversion

Rajendra S. Dhayal,* [¥] Werner E. van Zyl,* [‡] and C. W. Liu* [†]

Received 00th January 20xx,
Accepted 00th January 20xx

DOI: 10.1039/x0xx00000x

www.rsc.org/

Hydrogen is seen as an increasingly important clean and sustainable energy source going into the future. There are a host of materials being investigated for the storage of hydrogen. In this frontier, we provide an overview of hydride clusters derived from earth-abundant copper being used for the storage and conversion of hydrides into hydrogen, and the reaction of CO_2 with hydride sources to produce the formic acid/formate pairing, which are considered excellent hydrogen carriers. We summarize the main synthesis methods to stabilize high-nuclearity hydride clusters with phosphine, N-heterocyclic carbene, and in particular phosphor-1,1-dithiolate ligands. Unprecedented structures and hydride geometries have been revealed through both X-ray and neutron single crystal analyses. We point to the release of hydrogen in such hydride clusters through solar irradiation, thermolysis and acid treatments. Finally, we show the facile formation of rhombic nanoparticle copper morphologies derived from accurately determined high-nuclearity clusters and suggest this could provide a mechanism that links molecular structures with bulk microstructures of materials.

Introduction

The continuous growth of the human population coupled with expanding industrial sectors results in an increase in a global energy demand.[1] In order to sustain the increasing demand, energy systems need to become cost-effective and sustainable.[2] The depletion of fossil fuels and associated emission of greenhouse gases have been implicated in climate change issues and therefore the development and improvement of energy systems from renewable and sustainable sources are simultaneously a great scientific challenge and opportunity.[3] Sustainable and renewable sources include solar, wind, wave and geothermal energy. Although solar and wind energy are dependent on weather conditions, sunlight is generally regarded as the only long-term carbon-neutral resource for all global energy requirements. For example, assuming only 10% efficiency and covering less than 2% of the Earth's surface, the sun provides about 50 TW energy, satisfying all energy requirements well into the 21st century.[4]

However, regardless of the source, storage and transportation of energy from known renewable systems still remains a major challenge.[5] Hydrogen fuel-based technologies have emerged as a strong contender because it is considered a promising energy carrier, capable of storing and delivering energy in usable form[6] and can be utilized in a wide variety of applications.[7] Hydrogen storage materials should comply with a multitude of criteria that includes amongst others being lightweight, inexpensive and readily available, have high volumetric and gravimetric densities, rapid sorption kinetics, and easy activation.[8-12] A wide range of materials have been tested for H_2 gas storage, including metal hydrides,[13] complex hydrides,[5,14] chemical hydrides,[15] carbon materials,[16] and sorbents such as metal-organic frameworks (MOFs).[17] The main goal of H_2 storage materials[18,19] is to find materials that adsorb hydrogen with a H_2 density greater than the density of liquid H_2 which is only 70.8 kg m^{-3} at 20 K and 1 atm pressure.

The interstitial metal hydrides (MH_x) comprise the d- (especially Pd) and f-block metals (and alloys) and have received significant attention due to reversible hydrogen storage under ambient conditions, but unfortunately the gravimetric hydrogen storage

[†]Department of Chemistry, National Dong Hwa University, Hualien, Taiwan 97401
E-mail: chenwei@mail.ndhu.edu.tw
[‡]School of Chemistry and Physics, University of KwaZulu Natal, Westville Campus, Durban 4000, South Africa
E-mail: vanzylw@ukzn.ac.za
[¥]Department of Chemical Sciences, School of Basic and Applied Sciences, Central University of Punjab, Bathinda 151 001, India.
E-mail: rajendra.dhayal@cup.edu.in

Rajendra Singh Dhayal *received his B. Sc. and M.Sc. degree in chemistry from University of Rajasthan Jaipur and obtained his PhD degree from Indian Institute of Technology Madras. He was a postdoctoral fellow in group of Prof. Chen-Wei Liu at National Dong Hwa University and is currently Assistant Professor at Central University of Punjab.*

Chen-Wei Liu, received his PhD degree in 1994 from Texas A & M University, is currently a distinguished professor at the National Dong Hwa University in Taiwan. His research group has been focused on the synthesis of group 11 metal clusters and their alloys stabilized by dichalcogenolate ligands. He is also interested in the development of luminescent nanoscale materials.

View Article Online
DOI: 10.1039/C8DT04639E

Dalton Transaction

FRONTIER

density is low.[20] The light metal hydrides such as solid $[MgH_2]_\infty$ are amongst the best class of hydrogen storage materials but following decades of research, as a class, they are limited to a reversible hydrogen storage capacity of only 2 mass% at <373 K and 2 atm.[21] Complex hydrides have received much attention because many of them have appreciable gravimetric hydrogen storage capacities. In such hydrides the hydrogen atoms are covalently bonded to a central atom in an anion complex (e.g. $[AlH_6]^{3-}$, $[AlH_4]^-$, $[BH_4]^-$, $[NH_2]^-$) and stabilized by a cation, typically an alkali (e.g. Li) or alkaline earth metal (e.g. Mg) or a transition metal (e.g. Zn).[22] In particular, magnesium borohydride, $Mg(BH_4)_2$, consists of numerous phases[8] and is a potential solid-state hydrogen storage material with a very high gravimetric hydrogen content of 14.9 wt% H_2. A new cubic nanoporous polymorph, γ-$Mg(BH_4)_2$, has 33% empty space in the structure and reveals a remarkable volume collapse of 44% upon compression.[23] Recently, the system $Ca(BH_4)_2$–Mg_2NiH_4 was used to prove the possibility to fully reverse the borohydride decomposition process even in cases where the decomposition reaction leads to undesired stable boron containing species; the system has implications in understanding dehydrogenation and rehydrogenation reaction mechanisms.[24]

Werner E. van Zyl *is Professor of Chemistry at the University of KwaZulu-Natal, South Africa. He received BScHons and MSc degrees in South Africa, and a PhD degree (1998) in inorganic chemistry from Texas A&M University, USA, followed by postdoctoral work (1999-2003) in the Inorganic Materials Science group and MESA+ Research Institute at the University of Twente, The Netherlands. His current research interests include biomass usage and conversions, water purification and desalination processes, the fabrication of transparent and flexible solar cells, and metal hydride clusters.*

MOFs are promising hydrogen storage materials and have been extensively studied. MOFs are crystalline materials and are synthesized from metal ions and organic building blocks. As a result, a host of chemico-physico properties such as reactivity, framework topology, pore size, and surface area can be readily tuned by the selection of molecular building blocks leading to defined structures, permanent porosity, and high specific surface areas. Amongst the highest excess H_2 storage capacity within a MOF is 99.5 mg g^{-1} at 56 bar and 77 K in NU-100 which has a total capacity of 164 mg g^{-1} at 77 K and 70 bar,[25] and the highest total H_2 storage capacity reported is 176 mg g^{-1} (excess 86 mg g^{-1}) in MOF-210 at 77 K and 80 bar.[26] Recently, Long and co-workers reported the volumetric H_2 storage capacities over a range of near-ambient temperatures relevant to on-board storage. Based upon adsorption isotherm data, Ni_2(*m*-dobdc) (dobdc = dioxido-1,3-benzenedicarboxylate) was found to be the top-performing physisorptive storage material with a usable volumetric capacity between 100 and 5 bar of 11.0 g/L at 25 °C and 23.0 g/L with a temperature swing between −75 and 25 °C.[27]

A class of compounds typically not considered in the storage and conversion of hydrogen are high-nuclearity transition-metal hydride clusters. The omission is presumably due to the low gravimetrical and volumetric hydrogen densities such clusters obviously possess. However, given the large number of criteria needed (see above) for efficient hydrogen storage, it remains to be seen which combination of properties will trump others for specific applications. For example, the coinage metals Cu, Ag and Au have a richly associated photochemistry, and can release hydrogen (and other small gaseous molecules) under certain solar irradiation conditions, not readily achieved by other hydride systems that rely on thermal activation. In this frontier, we focus on the synthesis of copper hydrido clusters, followed by their H_2 storage and reactivity, CO_2 reduction and reactivity (formic acid is regarded as an excellent hydrogen carrier),[28] and finally the conversion into distinctively shaped nanoparticles.

Formation of copper hydride clusters

I. Phosphine ligands

Coinage metals hydrides have garnered significant interest owing both to their structural diversity and reactivity.[29,30] Phosphine ligands form a variety of different nuclearity copper hydride clusters like binuclear to tetranuclear,[31-34] and octanuclear,[35-36] having (μ_2/μ_3-H) mode of hydride as shown Figure 1(a-j). Among these clusters, only the hexameric $[HCuP(p\text{-tolyl})_3]_6$ was studied by single-crystal neutron diffraction to locate the exact hydride (μ_3-H) positions at triangular faces of octahedron.[37-39] A type of μ_6-H coordination was also observed during C-H activation (Figure 1k).[40]

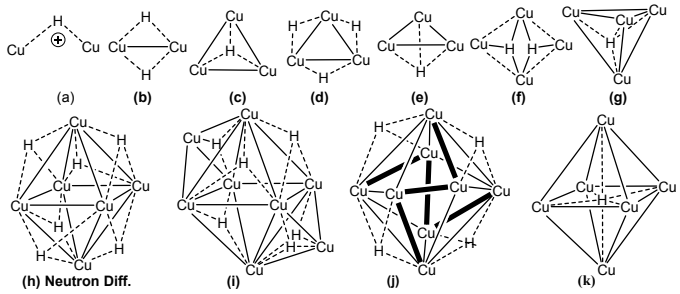

Figure 1. Different Cu core structures with predicted location of hydrides.

II. NHC ligands

The isolation of monoligated dimeric copper hydride using the NHC ligand was reported, Figure 1a-b.[41] Improved stability was obtained with 6- and 7- membered cyclic (alkyl)(amino)carbene (CAAC) ligands[42] and several dimers with bridging (μ_2-H) hydrides have been found to be stable at RT.[43] Recently, a bulky NHC ligand, 1,3-bis[2,6-bis[di(4-^{t}butylphenyl)methyl]-4-methylphenyl]imidazole-2-ylidene) (IPr) was used for a monomeric copper hydride (IPrCuH) with equilibrium of dimeric $[LCuH]_2$ in solution.[44]

III.Phosphor-1,1 dichalcogen ligands

In solution, cubic $[Cu_8\{E_2P(O^iPr)_2\}_6]^{2+}$ (E = S, Se) clusters react with a hydride source to form a hydride-centered tetracapped tetrahedral $[Cu_8(\mu_4\text{-}H)\{E_2P(O^iPr)_2\}_6]^+$ cluster, Figure 2A-B.[45] Ion trapping (halides, chalcogenides) within the empty $[Cu_8L_6]^{2+}$ system was achieved by the Liu group[46,47] and reaction of $[Cu_8(\mu_4\text{-}H)\{S_2CN^iPr_2\}_6]^+$ with one equivalent $[BH_4]^-$, excised a Cu atom and produced a neutral and hydride centered tricapped tetrahedral $[Cu_7(\mu_4\text{-}H)\{S_2CN^iPr_2\}_6]$ cluster, Figure 2C. An appropriate stoichiometric ratio of Cu^+ salt, dichalcogen (S/Se) ligands with excess (~1.5 equivalent) borohydride produced symmetric $[Cu_{20}H_{11}\{S_2P(O^iPr)_2\}_9]$,[47,48] $[Cu_{28}(H)_{15}(S_2CNBu_2)_{12}](PF_6)$,[49-50] $[Cu_{32}(H)_{20}\{S_2P(O^iPr)_2\}_{12}]$,[51-52] and asymmetric $[Cu_{20}H_{11}\{Se_2P(O^iPr)_2\}_9]$,[53] polyhydrido copper nanocluster (Figure 2D-G). The neutron diffraction study of these clusters revealed capping μ_3-H and interstitial (μ_4-H, μ_5-H, μ_6-H) hydride ligands.

Cu_{18} with encapsulation of a Cu_2 unit within C_{3h} symmetry, Figure 2D. The single-crystal neutron diffraction study revealed 11 hydride ions within the Cu_{20} core and displayed three different coordination modes: six μ_3-hydrides in capping mode on triangular-faces of both cupolae except apical triangles, two μ_4-hydrides in a tetrahedral cavity within cupolas, and three μ_4-hydrides in near square-planar geometry created by

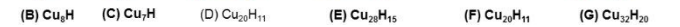

Figure 2. Dichalcogen (removed for clarity) and hydride (red, neutron diffraction) ligands stabilized copper (blue) frameworks; (A) Cubic core. (B) Tetracapped tetrahedral Cu_8H core (C) Tricapped tetrahedral Cu_7H core (D) Elongated triangular orthobicubola with encapsulation of Cu_2 unit create $Cu_{20}H_{11}$ (E) Rhombicuboctahedron Cu_{24} encapsulated tetrahedral Cu_4 to create $Cu_{28}H_{15}$ core (F) Asymmetric $Cu_{20}H_{11}$ core (central cuboctahedron Cu_{13} combines with a Cu_6 cupola and a single Cu atom). (G) A hexacapped rhombohedron (pink) of 14 Cu atoms sandwiched between two triangular cupolae of (2x9) Cu atoms.

Hydrogen storage

A hydrogen evolution study was performed from higher nuclearity (Cu_{20}, Cu_{28} and Cu_{32}) hydrides under different physico-chemical conditions including solar irradiation, thermolysis, and acidification, Figure 3.[47,49,53] These hydrides are excellent models for H_2 storage as they are stable in air and moisture and release hydrogen under mild conditions. Variable-temperature (VT) ^{1}H, ^{2}H NMR and ^{31}P NMR studies showed that heating of $Cu_{20}H_{11}$ (at ~65 °C), $Cu_{28}H_{15}$ (at ~70 °C) and $Cu_{32}H_{20}$ (at ~60 °C) clusters decomposes into $[Cu_7HL_6]^+$ or $[Cu_8HL_6]^+$ clusters with liberation of H_2 (δ = 4.61 ppm), {D_2, δ = 4.59 ppm} after 20 minutes, with concomitant deposition of Cu_2S.[47] The H_2 evolution was also monitored by GC analysis equipped with thermal conductivity detector (TCD). The clusters also liberated H_2 under solar irradiation (1 h), and entirely decomposed to the $[Cu_8HL_6]^+$ cluster when raising the temperature to approximately 42-44 °C. It was observed that the H_2 evolution rate is slower under sunlight irradiation than under thermolysis. Cluster $Cu_{28}H_{15}$ is capable of releasing 2.6, 4.0, 2.0, and 12.2 equivalents of H_2 per molecule exposed to solar energy, to reflux, or in the presence of weak- or strong acid, respectively, Figure 3A.[53] Cluster $Cu_{32}H_{20}$ is capable of releasing ~7, ~4, ~11 and ~19 equiv. of H_2 per molecule exposed to solar energy, to reflux, or in the presence of weak (12 h) and strong (5 min.) acids and converted into $Cu_8(Cl)\{S_2P(O^iPr)_2\}_6]^+$ and $Cu_8(H)\{S_2P(O^iPr)_2\}_6]^+$, respectively. The $[Cu_8(Cl)\{S_2P(O^iPr)_2\}_6]^+$ cluster can be converted into $Cu_8(H)\{S_2P(O^iPr)_2\}_6]^+$ using one molar equiv. of $[BH_4]^-$. Thus, with respect to hydrogen density, $Cu_{32}H_{20}$ is able to release ~0.30, ~0.17, ~0.48, ~0.85 wt% of H_2 under solar energy, thermolysis, or in the presence of weak and strong acid, respectively, Figure 3B. By comparison, the maximum H_2 density released from $Cu_{20}H_{11}$ was 0.50 wt% while interacting with strong acid. With thermolysis and solar irradiation $Cu_{20}H_{11}$ was converted into $[Cu_7HL_6]$ with liberation of H_2, while Cu_7H is convertible into Cu_8H. Finally, the corresponding Cu_{20}, Cu_{28} and Cu_{32} can be recovered from the yielded product $[Cu_8(H)\{L\}_6]^+$ or $[Cu_7(H)\{L\}_6]$ with further reaction of $[BH_4]^-$ to complete the H_2 evolution cycle. The complex $[Cu_8(H)\{S_2CN^nPr_2\}_6]^+$ releases H_2 in presence of $Ce(NO_3)_6^{2-}$ and is converted into $[Cu(S_2CN^nPr_2)_2]$.[54] The deuterated analogues $Cu_{20}D_{11}$, $Cu_{28}D_{15}$ and $Cu_{32}D_{20}$ were also reacted with HCl in an NMR tube, and a triplet at ~4.58 ppm and a doublet at 4.70 ppm were observed in the ^{1}H NMR and ^{2}H NMR spectra, respectively, thus confirming the hydridic state of hydrogen atom within the copper cores. In the gas phase, the chiral cores of nanoclusters $[Cu_{18}H_{16}(dppe)_5]^{2+}$ and $[Cu_{16}H_{14}(dppa)_5]^{2+}$ (or their deuterated analogues) indicated the evolution of H_2/D_2 and yielded corresponding $[Cu_{18}(L)_5]^{2+}$ and $[Cu_{16}(L)_5]^{2+}$ clusters of mixed (Cu^I/Cu^0) valence nanoclusters.[55] Heating of $[Cu_{18}H_{16}(dppe)_5]^{2+}$ at 55 °C in VT ^{1}H NMR shows H_2 (δ = 4.62 ppm) evolution in $CDCl_3$ solution. In 2014, the Van Leeuwen group reported H_2 evolution from nanocluster $[Cu_{18}H_7\{S(C_6H_4)PPh_2\}_{10}]I$ (4 mg, 0.02 mmol) in THF *via* visible light, thermolysis and acidifications and produced 27 µL (0.0001 mmol) H_2 under visible light.[56] Unfortunately, hydrogen evolution induced by copper hydrides and proposed in Figure 3 are not catalytic due to the intrinsic difficulty in hydride replenishment. An alternative hydride source such as hydrides from proton reduction seems feasible. However, the controlled experiment of proton reduction in solution will be very difficult to proceed due to the hydridic characteristics of these copper hydrides. Nevertheless, it can be performed under electrochemical conditions by using $Cu_{32}H_{20}(dtp)_{12}$ as the catalysts (TOF of 16 mol. sec^{-1} at overpotential of 0.6 V).[57]

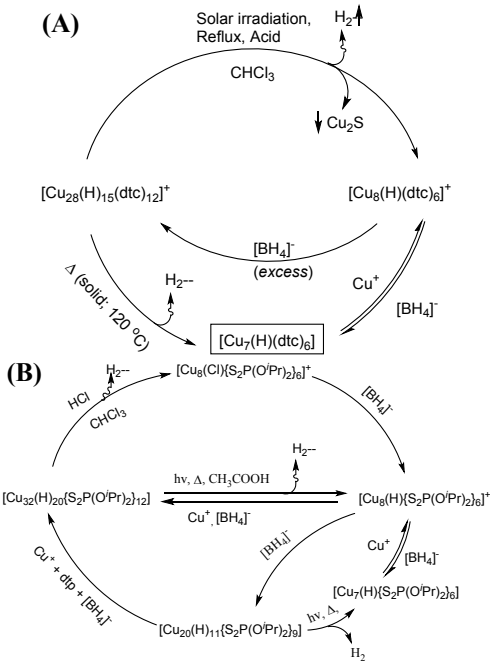

Figure 3. Proposed H_2 evolution cycle (A) from $Cu_{28}H_{15}$ and (B) from $Cu_{32}H_{20}$ and $Cu_{20}H_{11}$ with inter conversion with corresponding Cu_8H and Cu_7H.

Reactivity with CO_2 and the formic acid/formate pairing

Energy-rich products such as formic acids (usually trapped as formate ion)[58] are an attractive target for energy storage during hydrogenation of CO_2. These fuels can be stored and transported more efficiently compared to an equal quantity of CO_2 first taken up and then emitted over the life cycle of fuel.[59] Copper hydrides can react stoichiometrically with CO_2 to produce formate and formic acids. Noteworthy is that NHC ligands prefer formation of formate, while phosphine and dichalcogen containing copper hydrides prefer formic acid.

A mononuclear [(IPr)CuH] complex was formed from a reaction between [(IPr)Cu(O^{t}Bu)] and $(EtO)_3SiH$, and subsequent insertion of CO_2 into the Cu-H bond at RT yielded the corresponding copper formate [(IPr)CuO_2CH] in 81% yield, Scheme 1.[60] Further addition of $(EtO)_3SiH$ into the copper formate solution releases the silyl formate and regenerates the copper hydride [(IPr)CuH] catalyst.

Scheme 1. NHC ligated copper formate formation.

Generally, the reactivity of any metal hydride toward CO_2 depends on the degree of anionic character at hydrogen. The $[(IPrCu)_2(\mu\text{-}H)]^+$ complex displays considerable hydridic character despite its overall positive charge and CO_2 and acetylene reacts readily with $[(IPrCu)_2(\mu\text{-}H)]^+$ to form $[(IPrCu)_2(\mu\text{-}O_2CH)]^+$ and a (*trans*-phenyl vinyl)-bridged dicopper(I) complex, Scheme 2.[61] The 6- and 7- membered NHC ligand stabilizing the dinuclear $[CuHL]_2$ species showed rapid insertion of CO_2 to yield the corresponding formate complex.[43]

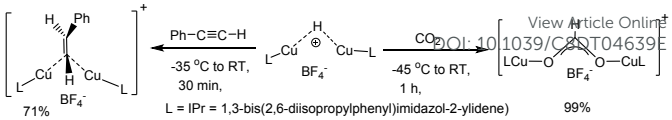

Scheme 2. Synthesis and reactivity of hydrido-bridged dicopper cation.

$[Cu_2(\mu\text{-}H)(\mu\text{-dpmpppm})_2]^+$ was exposed to CO_2 (1 equiv.) at RT and readily formed $[Cu_2(\mu\text{-HCOO})(\mu\text{-dpmpppm})_2]^+$ in 78% yield, Scheme 3.[62] The reaction of the formate-bridged Cu complex in acidic medium released 1 equiv. of HCOOH, and further addition of $[BH_4]^-$ to $[Cu_2(\mu\text{-dpmpppm})_2]^{2+}$ or $[Cu_2(\mu\text{-Cl})(\mu\text{-dpmpppm})_2]^+$ yielded the original $[Cu_2(\mu\text{-H})(\mu\text{-dpmpppm})_2]^+$. Similarly, $[Cu_4(\mu\text{–}H)_2(\mu_4\text{–}H)(\mu\text{–dpmpppm})_2]^+$ also reacted with CO_2 (1 atm, 25 ºC) to yield $Cu_4(\mu\text{–HCOO})_3(\mu\text{–dpmpppm})_2]^+$ in 69 % yield, which subsequently react with HCl to yield $[Cu_4(\mu\text{–Cl})_3(\mu\text{–dpmpppm})_2]^+$ along with 3 equivalent formic acid.

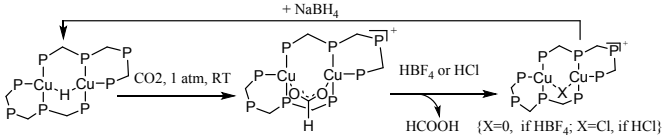

Scheme 3. Dpmppm ligated copper formate stabilization and formation of HCOOH.

The copper hydride cluster $[Cu_{14}H_{12}(phen)_6(PPh_3)_4]^{2+}$, which was isolated by reaction of $[(Ph_3P)CuH]_6$ with 1,10-phenanthroline, reacts with CO_2 in the presence of excess Ph_3P to form a formate complex, $[(Ph_3P)_2Cu(\eta^2\text{-}O_2CH)]$ along with $[(phen)(Ph_3P)CuCl]$.[63] A similar formate complex $[(Ph_3P)_2Cu(\eta^2\text{-}O_2CH)]$ was also observed from the reaction of $[(Ph_3P)CuH]_6$ with CO_2 in presence of 6 equiv $[P(Ph)_3]$.[64] Hydrogenolysis (H_2, 1 atm.) of the Cu-O bond of (CuO-^{t}Bu)$_4$ in THF under mild conditions (23°C, 5 h) in the presence of a stoichiometric amount (1 mol/mol of Cu) of tridentate MeC(CH_2PPh_2)$_3$ 'tripod', yielded the dimeric complex $[HCu(tripod)]_2$ in 75% yield, Scheme 4,[33] which was thermally unstable in toluene solution above at 40°C. The tripod-type ligands typically provide an appropriate coordination sphere around the copper(I) center in order to accommodate a fourth ligand. For example, the hydride dimer was reacted with 1 atm of CO_2 in toluene at 25 °C and immediately deposited monomeric (η^3-tripod)Cu(η^1-O_2CH) in 89% yield.

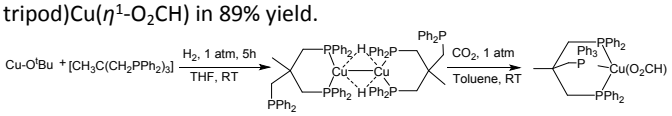

Scheme 4. Synthesis of tridentate ligated MeC(CH_2PPh_2)$_3$ copper formate.

In 2015, the Appel group used the base 1,8-diazabicyclo[5.4.0]undec-7-ene (DBU) to form $[(tripod)Cu\text{-}DBU]^+$ and reacted it with H_2 which formed a transient intermediate [(η^3-tripod)CuH], which subsequently reacted with CO_2 to form a η^1 coordinated formate complex $[(tripod)Cu\text{-}O_2CH]^+$, Scheme 5.[65] The formate ligand is rapidly displaced by excess DBU, facilitating turnover and generating the free formate product. The Ikariya group reported a Cu DBU complex for hydrogenation (H_2) of CO_2 to give [DBU-H] and $[HCO_2]^-$ via a monomeric copper hydride intermediate.[66] A hydride-bridged dimer $[(LCu)_2H]^+$ was structurally characterized during the

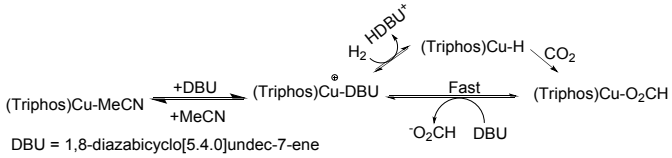

Scheme 5. The formate formation recycle CO_2 in presence of triphos CuH and DBU.

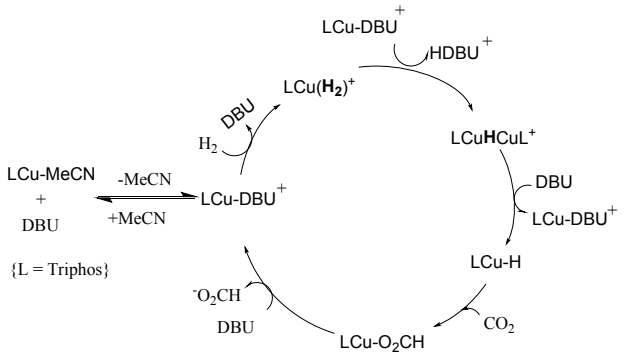

Figure 4 Extended recycling for CO_2 conversion into formate in the presence of triphos CuH and DBU

hydrogenation of CO_2 in the presence of DBU and proposed a mechanism, Figure 4.[67] Recently,[68] the Bertrand group demonstrated that a CAAC/NHC ligated mononuclear copper hydride work in tandem with Lewis pairs [DBU][BR_3] for reduction of CO_2 to formate using H_2. Initial insertion of CO_2 into the CuH bond gave a copper formate (Scheme 6). The C-O bond of the copper formate was cleaved by H_2, which was activated by the Lewis pair, returning the copper hydride complex and formate salt [HDBU][HCO_2^-]. This catalytic cycle involved the synergistic effect between L − Cu − H and [DBU][BR_3] for reduction of CO_2 with H_2. A Lewis pair having a less steric hindered base and more acidic borane in the presence of CAAC-Cu-H (0.00025 mmol) achieved the best CO_2 conversion to formate (TONs 1881).

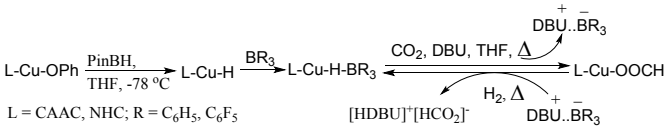

Scheme 6. CO_2 reduction cycle in presence of LCuH , H_2 and classical Lewis pair.

He and co-workers described a gas-phase reaction of the anion $[Cu_2H_2]^-$ with CO_2 at variable temperatures (298-559 K) and observed that increased reaction temperature switched the product formation of $[Cu_2H_2CO_2]^-$ at room temperature to $[CuH_2CO_2]^-$ at 559 K, indicating the possible formation of stable formate species in $[CuH_2CO_2]^-$.[69] The DFT study supported the direct hydride transfer from $[Cu_2H_2]^-$ to the C atom of CO_2 to be the most favorable pathway for the C–H bond formation in the gas phase. By comparing anions $[Cu_2H_3]^-$ and $[CuH_2]^-$, it was found the latter was more reactive with CO_2 to produce formate under a gas phase conditions.[70]

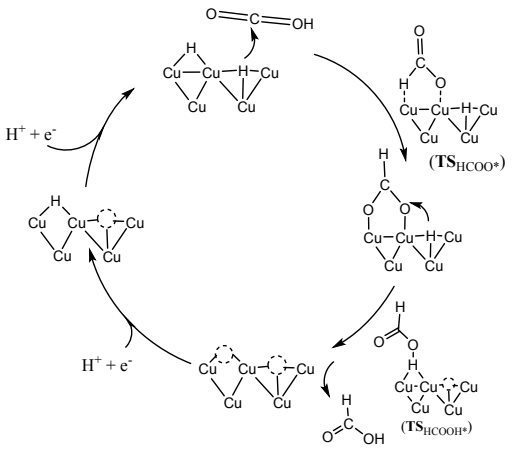

Figure 5 Lattice hydride mechanism for electrocatalytic reduction of CO_2 into HCOOH using $[Cu_{32}(H)_{20}\{S_2P(O^iPr)_2\}_{12}]$ at low overpotentials.

View Article Online
DOI: 10.1039/C8DT04639E

For a mechanistic understanding of CO_2 reduction on nanostructure Cu catalyst, a structurally precise ligand-protected copper hydride nanocluster $[Cu_{32}(H)_{20}\{S_2P(O^iPr)_2\}_{12}]$ was studied and electrocatalytic CO_2 reduction at low overpotential performed, Figure 5.[57] The DFT study supported a negative charge on μ_3-H capping hydrides is most favourable to react with C atoms of CO_2 molecules, which favours formation of HCOOH to generate the [$Cu_{32}H_{19}L_{12}$-HCOO] species and then the positive charge of Cu atoms stabilized the [$Cu_{32}H_{19}L_{12}$-OOCH] species. The next step involve the addition of adjacent μ_4-H to release HCOOH product and the sequential vacancies of two lattice hydrides within the copper core readily re-establish via two sequential proton-reduction steps, Figure 5. It was also predicted that if a lattice hydride initially interacts with O rather than C of CO_2 then CO will be produced over the HCOOH formation. The main reason for the formation of HCOOH over the CO using the Cu_{32} nanocluster appears to be that CO formation needs higher activation energy. The S and P atoms of ligands are not playing any direct role to CO_2 reduction for this cluster. It indicates that the Cu framework of the nanocluster remain stable until it regains the lost hydrides to produce HCOOH. Along with the CO_2 electoreduction, the hydrogen evolution reaction (HER) can also be a major competing reaction. But HCOOH formation is kinetically preferred over the HER due to low overpotential, but the higher potential will greatly favour for HER.

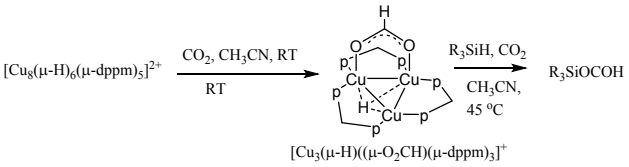

Scheme 7. A tricopper formate synthesis from Cu_8H_6 core and CO_2, and hydrosilylation.

Recently, a reaction of copper hydride cluster $[Cu_8(\mu\text{-}H)_6(\mu dppm)_5]^{2+}$ with CO_2 (1 atm, RT) afforded a tricopper complex, $[Cu_3(\mu\text{-}H)(\mu\text{-}O_2CH)(\mu\text{-}dppm)_3]^+$, Scheme 7, and its existence was confirmed by the solid state structure followed by an NMR study.[36] Further, the reaction of Cu_8H_6 with CO_2 forming a tricopper hydride was also performed for hydrosilylation (Me_2PhSiH/$MePh_2SiH$) to yield corresponding silylformate ($R_3SiOCOH$). Recently, the Crimmin group characterized the heterobimetallic hydride Au–H–Cu, which acts as a pre-catalysts for the conversion of CO_2 to HCO_2Bpin using HBpin as a reductant.[71]

Conversion into nanoparticles and alloy clusters

The sequential reaction of $[BH_4]^-$ with $[Cu_{20}H_{11}]$ yielded $[Cu_{32}H_{20}]$ and subsequently unique rhombus-shaped copper nanoparticles, which indicated the existence of many polyhydrido metal clusters as intermediates prior to formation of nanoparticles of various metals under wet chemical methods.[52,53] A superatom with centred Cu_{13} core of icosahedron $[Cu_{25}H_{22}(PPh_3)_{12}]^+$,[72] and cuboctahedron $[Cu_{13}(S_2CN^nBu_2)_6(C{\equiv}CR)_4](PF_6)$ (R=C(O)OMe, C_6H_4F),[73] $[Au/Ag@Cu_{12}(S_2CN^nBu_2)_6(C{\equiv}CPh_4)_4][CuCl_2]$ was isolated, Figure 6.[74] Interestingly, the central copper was also replaced by halogen/chalcogen atoms to obtain copper clusters containing main group elements (Cl, Br, S) with a hyper-coordination number 12 and which show enhanced luminescence properties.[75-76]

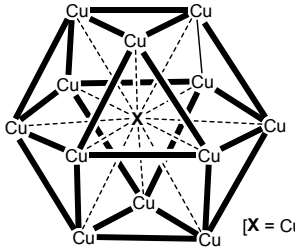

Figure 6. Miniature of bulk fcc structure, Cu/Ag/Au/S/Cl/Br@Cu_{12} (cuboctahedral) core.

Conclusions and outlook

The dichalcogen stabilized polyhydrido copper nanoclusters reveal exceptional stability in air and moisture in comparison to phosphine and NHC ligated copper hydrides. The NHC ligands are able to stabilize lower nuclearity copper hydrides. Spectroscopically, it was shown that dimers show an equilibrium with mononuclear NHC-CuH and that is presumably the reason for quick reaction of these dinuclear copper hydrides with CO_2 at RT, but their isolation (mononuclear) at RT remains a challenge. Multidentate phosphine ligated copper hydrides have shown excellent reactivity with CO_2 to yield the formate product, which yielded HCOOH in acidic (HBF_4/HCl) medium. Dichalcogen stabilized polyhydrido copper (Cu_{20}, Cu_{28}, Cu_{32}) nanoclusters are stable in air and moisture, and reveals the presence of both interstitial and capping hydrides, which evolves as H_2 under mild thermolysis, solar irradiation and acidifications under a recycled process. Thus, these are excellent models for H_2 storage. The [$Cu_{32}H_{20}L_{12}$] cluster shows outstanding performance in synthesis of HCOOH from CO_2 at low overpotential with regeneration of original molecules. Thus copper hydrides are able to convert CO_2 into formate and formic acid (C_1 molecules) but generating molecules like CH_3OH, C_2H_5OH, etc. remain a challenge.

Conflicts of interest

There are no conflicts to declare.

Acknowledgements

Financial supports by Ministry of Science and Technology in Taiwan (MOST 106–2113-M-259-010) and Science and Engineering Research Board (YSS/2015/001105), Department of Science and Technology, India are gratefully.

Notes and references

1 N. S. Lewis and D. G. Nocera, *Proc. Natl. Acad. Sci.*, 2006, **103**, 15729–15735.
2 L. Shi and M. Y. L. Chew, *Renew. Sust. Energy Rev*., 2012, **16**, 192-207.
3 N. Armaroli and V. Balzani, *Angew. Chem. Int. Ed.*, 2007, **46**, 52–66.
4 T. R. Cook, D. K. Dogutan, S. Y. Reece, Y. Surendranath, T. S. Teets and D. G. Nocera, *Chem. Rev*., 2010, **110**, 6474-6502.
5 S. Orimo, Y. Nakamori, J. R. Eliseo, A. Züttel and C. M. Jensen, *Chem. Rev.* 2007, **107**, 4111-4132.
6 a) N.A.A. Rusman and M. Dahari, *Intl. J. Hydrogen Energy*, 2016, **41**, 12108-12126; b) N. Armaroli and V. Balzani, *ChemSusChem* 2011, **4**, 21–36.
7 L. Schlapbach, and A. Züttel, *Nature*, 2001, **414**, 353-8.
8 M. B. Ley, L. H. Jepsen, Y.-.S Lee, Y. W. Cho, J. M. Bellosta von Colbe, M. Dornheim, M. Rokni, J. O. Jensen, M. Sloth, Y. Filinchuk, J. E. Jørgensen, F. Besenbacher and T. R. Jensen, *Mater. Today*, 2014, **17**, 122-128.
9 A. Züttel, A. Borgschulte and L. Schlapbach, *Hydrogen as a Future Energy Carrier*, Wiley-VCH, Weinheim, Germany, 2008.
10 M. Hirscher, *Handbook of Hydrogen Storage: New Materials for Future Energy Storage*, Wiley-VCH, Weinheim, Germany, 2010.
11 G. S. Walker, *Solid-State Hydrogen Storage: Materials and Chemistry*, Woodhead Publishing Ltd, 2008
12 U. Eberle and R. von Helmolt, *Energy Environ. Sci.*, 2010, **3**, 689-699.
13 B. Sakintuna, F. Lamari-Darkrimb and M. Hirscher, *Int. J. Hydrogen Energy*, 2007, **32**, 1121-1312.
14 W. Grochala and P. P. Edwards, *Chem. Rev*., 2004, **104**, 1283-1316.
15 C. W. Hamilton, R. T. Baker, A. Staubitz and I. Manners, *Chem. Soc. Rev*., 2009, **38**, 279-293.
16 R. H. Baughman, A. A. Zakhidov and W. A. de Heer, *Science,* 2002, **297**, 787-792.
17 M. P. Suh, H. J. Park, T. K. Prasad and D.-W. Lim, *Chem. Rev*., 2012, **112**, 782–835.
18 J. Yang, A. Sudik, C. Wolverton and D. J. Siegel, *Chem. Soc. Rev*., 2010, **39**, 656-675.
19 R. E. Morris and P. S. Wheatley, *Angew. Chem. Int. Ed*., 2008, **47**, 4966-4981.
20 B. D. Adams and A. Cheng, *Mater. Today*, 2011, 14, 282-289
21 D. Mukherjee and J. Okuda, *Angew. Chem. Int. Ed.*, 2018, **57**, 1458-1473.
22 J. Graetz, *Chem. Soc. Rev*., 2009, **38**, 73–82.
23 W. I. F. David, S. K. Callear, M. O. Jones, P. C. Aeberhard, S. D. Culligan, A. H. Pohl, S. R. Johnson, K. R. Ryan, J. E. Parker, P. P. Edwards, C. J. Nuttall and A. Amieiro-Fonseca, *Phys. Chem. Chem. Phys*., 2012, **14**, 11800–11807.
24 N. Bergemann, C. Pistidda, C. Milanese, M. Aramini, S. Huotari, P. Nolis, A. Santoru, M. R. Chierotti, A.-L. Chaudhary, M. D. Baro, T. Klassen and M. Dornheim, *J. Mater. Chem. A*, 2018, **6**, 17929–17946.
25 O. K. Farha, A. O. Yazaydin, I. Eryazici, C. D. Malliakas, B. G. Hauser, M. G. Kanatzidis, S. T. Nguyen, R. Q. Snurr and J. T. Hupp, *Nat. Chem*., 2010, **2**, 944-948.
26 H. Furukawa, N. Ko, Y. B. Go, N. Aratani, S. B. Choi, E. Choi, A. O. Yazaydin, R. Q. Snurr, M. O'Keeffe, J. Kim and O. M. Yaghi, *Science,* 2010, **329**, 424-428.
27 M. T. Kapelewski, T. Runčevski, J. D. Tarver, H. Z. H. Jiang, K. E. Hurst, P. A. Parilla, A. Ayala, T. Gennett, S. A. FitzGerald, C. M. Brown and J. R. Long, *Chem. Mater*., DOI: 10.1021/acs.chemmater.8b03276.
28 M. Grasemann and G. Laurenczy, *Energy Environ. Sci*., 2012, **5**, 8171-8181.
29 R. S. Dhayal, W. E. van Zyl and C. W. Liu, *Acc. Chem. Res*., 2016, **49**, 86–95.
30 A. J. Jordan, G. Lalic and J. P. Sadighi, *Chem. Rev.,* 2016, **116**, 8318–8372.
31 G. V. Goeden, J. C. Huffman and K. G. Caulton, *Inorg. Chem*. 1986, **25**, 2484-2485.
32 A. W. Cook, T.-A. D. Nguyen, W. R. Buratto, G. Wu and T. W. Hayton, *Inorg. Chem*. 2016, **55**, 12435−12440
33 T. Nakajima, Y. Kamiryo, K. Hachiken, K. Nakamae, Y. Ura and T. Tanase, *Inorg. Chem*. 2018, **57**, 11005−11018
34 H.-H. Nie, Y.-Z. Han, Z. Tang, A.-Y. Yang and B. K. Teo, *J. Clust. Sci*. 2018, **29**, 837–846
35 T. H. Lemmen, K. Folting, J. C. Huffman and K. G. Caulton, *J. Am. Chem. Soc.,* 1985, **107**, 7774-7775
36 K. Nakamae, M. Tanaka, B. Kure, T. Nakajima, Y. Ura and T. Tanase, *Chem. Eur. J.* 2017, **23**, 9457 – 9461
37 R. C. Stevens, M. R. McLean and R. Bau, *J. Am. Chem. Soc.,* 1989, **111**, 3472-3473
38 S. A. Bezman, M. R. Churchill, J. A. Osborn and J. Wormald, *J. Am. Chem. Soc.,* 1971, **93**, 2063-2065.

39 C. Deutsch, N. Krause and B. H. Lipshutz, *Chem. Rev*. 2008, **108**, 2916-2927.
40 R. D. Köhn, Z. Pan, M. F. Mahon and G. Kociok-Köhn, *Chem. Commun.,* 2003, 1272-1273.
41 N. P. Mankad, D. S. Laitar and J. P. Sadighi, *Organometallics*, 2004, **23**, 3369−3371.
42 G. D. Frey, B. Donnadieu, M. Soleilhavoup and G. Bertrand, *Chem. - Asian J*. 2011, **6**, 402−405.
43 A. J. Jordan, C. M. Wyss, J. Bacsa and J. P. Sadighi, *Organometallics*, 2016, **35**, 613−616
44 E. A. Romero, P. M. Olsen, R. Jazzar, M. Soleilhavoup, M. Gembicky and G. Bertrand, *Angew. Chem. Int. Ed*. 2017, **56**, 4024 –4027.
45 (a) P.-K. Liao, B. Sarkar, H.-W. Chang, J.-C. Wang, and C. W. Liu, *Inorg. Chem.* 2009, **48**, 4089-4097 (b) C. W. Liu, B. Sarkar, Y.-J. Huang, P.-K. Liao, J.-C. Wang, J.-Y. Saillard and S. Kahal, *J. Am. Chem. Soc.* 2009, **131**, 11222-11233.
46 R.-S. Dhayal, J.-H. Liao, H.-N. Hou, R. Ervilita, P.-K. Liao and C. W.,Liu, *Dalton Trans*., 2015, **44**, 5898-5908
47 R. S. Dhayal, J.-H. Liao, Y.-R. Lin, P.-K. Liao, S. Kahlal, J.-Y. Saillard and C. W. Liu, *J. Am. Chem. Soc.* 2013, **135**, 4704-4707.
48 J.-H. Liao, R. S. Dhayal, X. Wang, S, Kahlal, J.-Y. Saillard and C. W. Liu, *Inorg. Chem.* 2014, **53**, 11140-11145.
49 A. J. Edwards, R. S. Dhayal, P.-K. Liao, J.-H. Liao, M.-H. Chiang, R. O. Piltz, S. Kahlal, J.-Y. Saillard and C. W. Liu, *Angew. Chem. Int. Ed.* 2014, **53**, 7214-7218.
50 P. V. V. N. Kishore, J.-H. Liao, H.-N. Hou, Y.-R. Lin, and C. W. Liu, *Inorg. Chem.* 2016, **55**, 3663−3673.
51 R. S. Dhayal, J.-H. Liao, S. Kahlal, X. Wang, Y.-C. Liu, M.-H. Chiang, W. E. van Zyl, J.-Y. Saillard and C. W. Liu, *Chem.- Eur. J.* 2015, **21**, 8369-8374.
52 R. S. Dhayal, H.-P. Chen, J.-H. Liao, W. E. van Zyl and C. W. Liu, *ChemistrySelect* 2018, **3**, 3603-3610.
53 R. S. Dhayal, J.-H. Liao, X. Wang, Y.-C. Liu, M.-H. Chiang, S. Kahlal, J.-Y. Saillard and C. W. Liu, *Angew. Chem. Int. Ed.* 2015, **54**, 13604−13608.
54 P.-K. Liao, C.-S. Fang, A.J. Edwards, S. Kahlal, J.-Y. Saillard and C.W. Liu, *Inorg. Chem*. 2012, **51** 6577–6591.
55 J. Li, H. Z. Ma, G. E. Reid, A.J. Edwards, Y. Hong, J. M. White, R. J. Mulder and R. A. J. O'Hair, *Chem.- Eur. J*., 2018, **24**, 2070 – 2074.
56 M. A. Huertos, I. Cano, N. A. G. Bandeira, J. Benet-Buchholz, C. Bo and P. W. N. M. Van Leeuwen, *Chem.- Eur. J.* 2014, **20**, 16121-16127.
57 Q. Tang, Y. Lee, D.-Y. Li, W. Choi, C. W. Liu, D. Lee and D.-E. Jiang, *J. Am. Chem. Soc*. 2017, **139**, 9728-9736
58 S. Enthaler, J. von Langermann and T. Schmidt, *Energy Environ. Sci.* 2010, **3**, 1207−1217.
59 M. Aresta, A. Dibenedetto and A. Angelini, *Chem. Rev*., 2014, **114**, 1709−1742.
60 L. Zhang, J. Cheng and Z. Hou, *Chem. Comm*. 2013, **49**, 4782-4784.
61 M. Wyss, B. K. Tate, J. Bacsa, T. G. Gray and J. P. Sadighi, *Angew. Chem. Int. Ed.,* 2013, **52**, 12920–12923
62 K. Nakamae, B. Kure, T. Nakajima, Y. Ura and T. Tanase, *Chem. Asian J.* 2014, **9**, 3106-3110
63 T. A. D. Nguyen, B. R. Goldsmith, H. T. Zaman, G. Wu, B. Peters and T. W. Hayton, *Chem.- Eur. J.* 2015, **21**, 5341-5344.
64 B. Beguin, B. Denise, R.P.A. Sneeden, *J. Organomet. Chem.* 1981, **208**, C18–C20.
65 C. M. Zall, J. C. Linehan and A. M. Appel, *ACS Catal*. 2015, **5**, 5301-5305.
66 R. Watari, Y. Kayaki, S.-I Hirano, N. Matsumoto and T. Ikariya, *Adv. Synth. Catal.* 2015, **357**, 1369-1373.
67 C. M. Zall, J. C. Linehan and A. M. Appel, *J. Am. Chem. Soc*. 2016, **138**, 9968-9977
68 E. A. Romero, T. Zhao, R. Nakano, X. Hu, Y. Wu, R. Jazzar and G. Bertrand, *Nature Catalysis,* 2018, **1**, 743–747.
69 Y.-Z. Liu, L.-X. Jiang, X.-N. Li, L.-N. Wang, J.-J. Chen, and S.-G. He, *J. Phys. Chem. C* 2018, **122**, 19379−19384.
70 A. Zavras, H. Ghari, A. Ariafard, A. J. Canty, and R. A. J. O'Hair, *Inorg. Chem.*, 2017, **56**, 2387–2399.
71 A. Hicken, A. J. P. White, and M. R. Crimmin, *Angew. Chem*., 2017, **56**, 15127-15130.
72 T.-A. D. Nguyen, Z. R. Jones, B. R. Goldsmith, W. R. Buratto, G. Wu, S. L. Scott and T. W. Hayton, *J. Am. Chem. Soc*., 2015, **137**, 13319−13324.
73 K. K. Chakrahari, J.-H. Liao, S. Kahlal, Y.-C. Liu, M.-H. Chiang, J.-Y. Saillard and C. W. Liu, *Angew. Chem. Int. Ed*. 2016, **55**, 14704 – 14708.
74 R. P. B. Silalahi, K. K. Chakrahari, J.-H. Liao, S. Kahlal, Y.-C. Liu, M.-H. Chiang, J.-Y. Saillard and C. W. Liu, *Chem. Asian J*. 2018, **13**, 500 – 504.
75 K. K. Chakrahari, R. P. B. Silalahi, J.-H. Liao, S. Kahlal, Y.-C. Liu, J.-F. Lee, M.-H. Chiang, J.-Y. Saillard and C. W. Liu, *Chem. Sci*. 2018, **9**, 6785–6795.
76 S. Sharma, K. K. Chakrahari, J.-Y. Saillard and C. W. Liu, *Acc. Chem. Res.*, 2018, **51**, 2475–2483.